

Modified figures for

The Weddell Gyre heat budget associated with the Warm Deep Water circulation derived from Argo Floats

Krissy Anne Reeve¹, Torsten Kanzow^{1,2}, Olaf Boebel¹, Myriel Vredenburg¹, Volker Strass¹, Rüdiger Gerdes^{1,3}

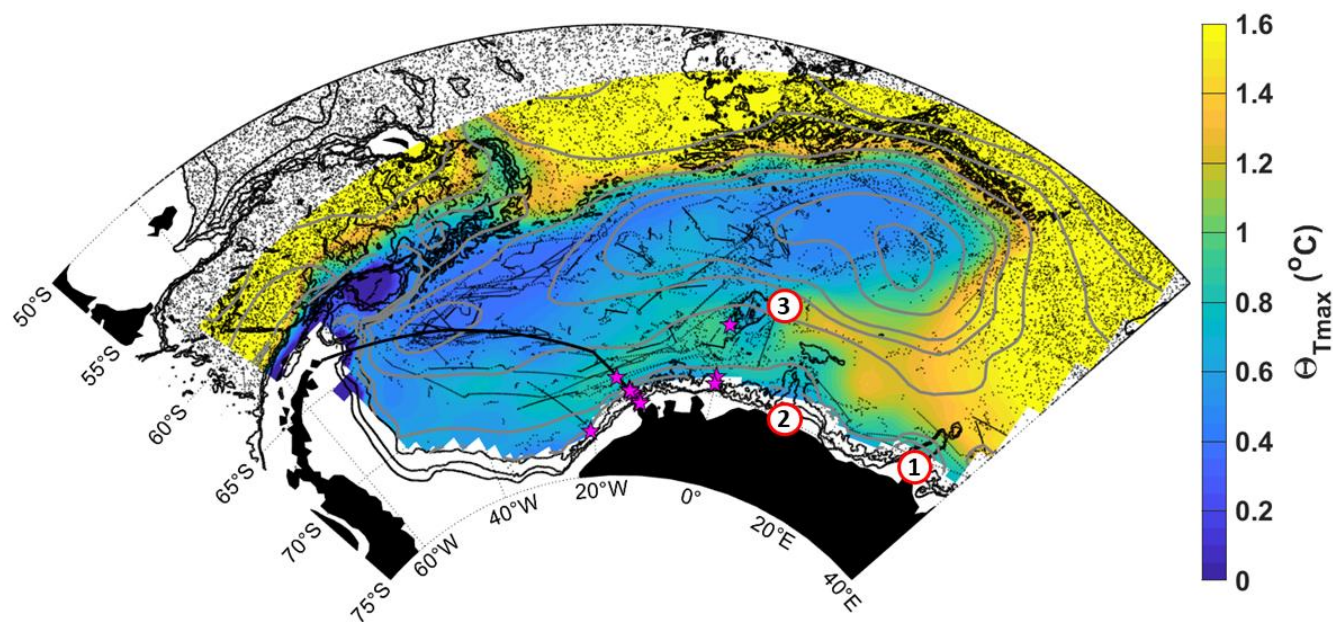


Figure 1: Sub-surface conservative temperature at the depth of temperature maximum (Θ_{max}) with streamlines (grey contours) of the vertically integrated stream function for 50-2000 dbar with a spacing of 5 Sv, derived from in-situ observations from Argo floats (Reeve et al., 2019, 2016). Black dots show Argo float profile positions and red stars show mooring positions used in velocity field estimates. The thick black line shows the repeat ship-based transect from Kapp Norvegia to Joineville Island. The red circles labelled 1-3 show (1) Gunnerus Ridge, (2) Astrid Ridge and (3) Maud Rise. The black contours show the 1000, 2000 and 3000 m isobaths, from the general bathymetric chart of the oceans (GEBCO, IOC et al., 2003).

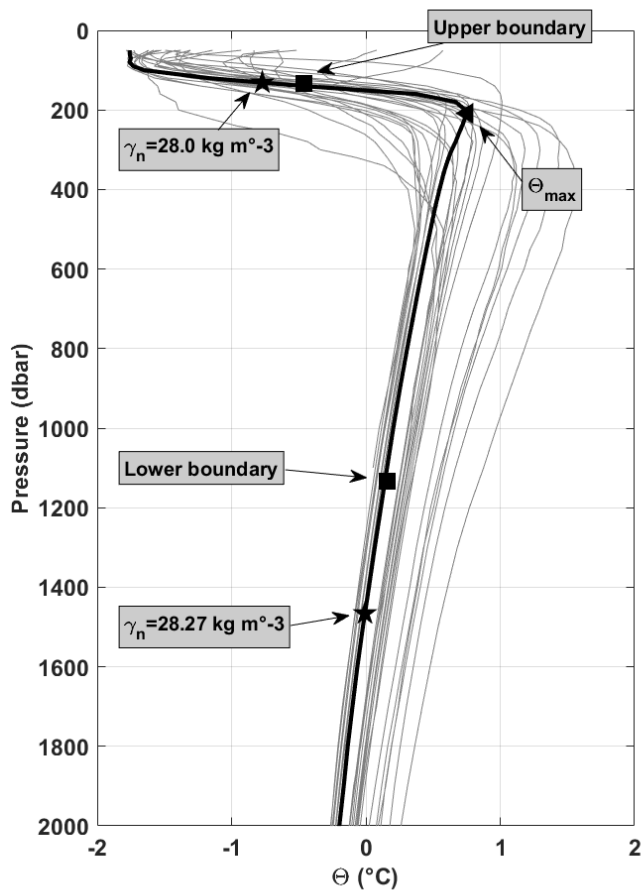
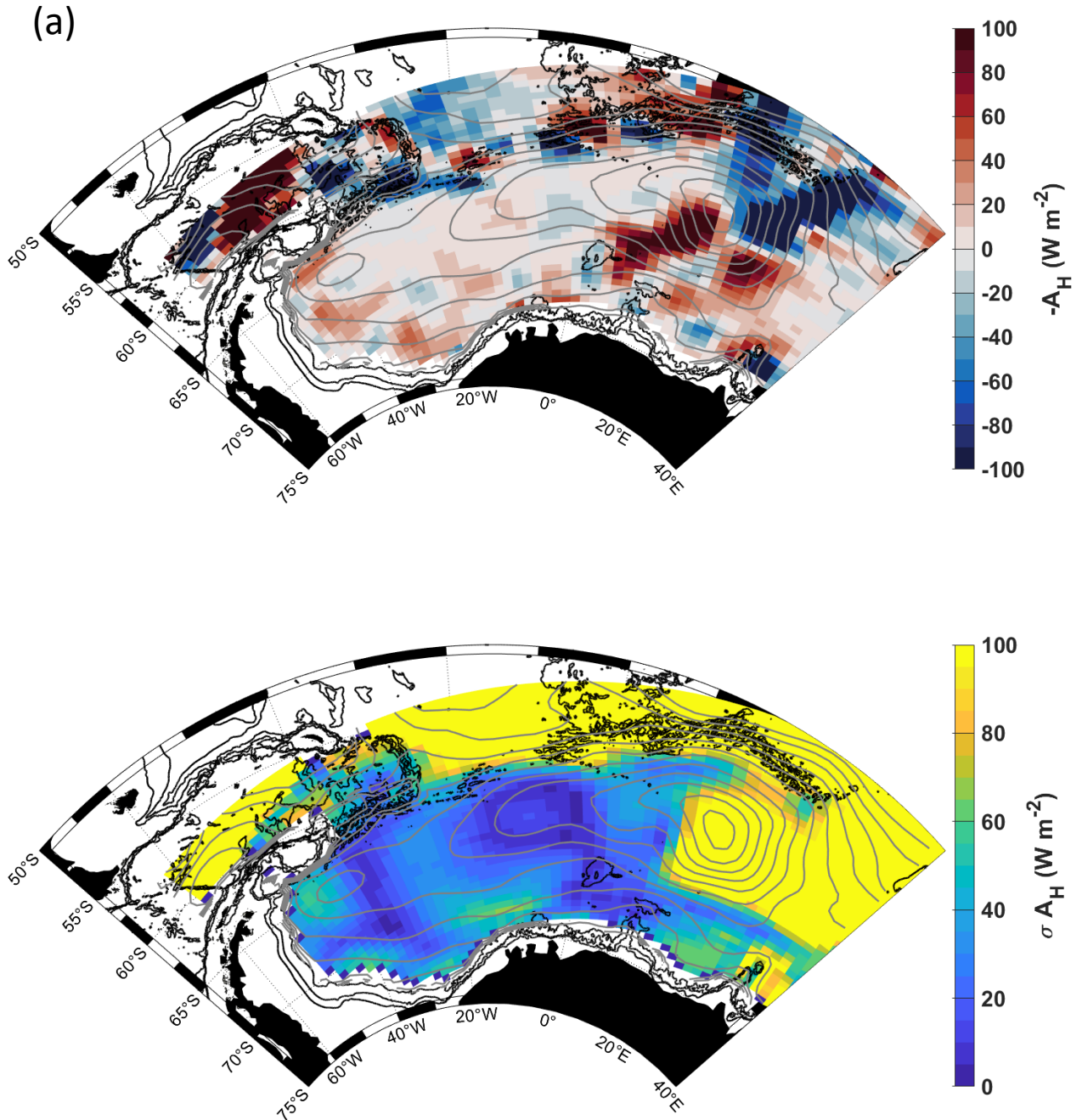
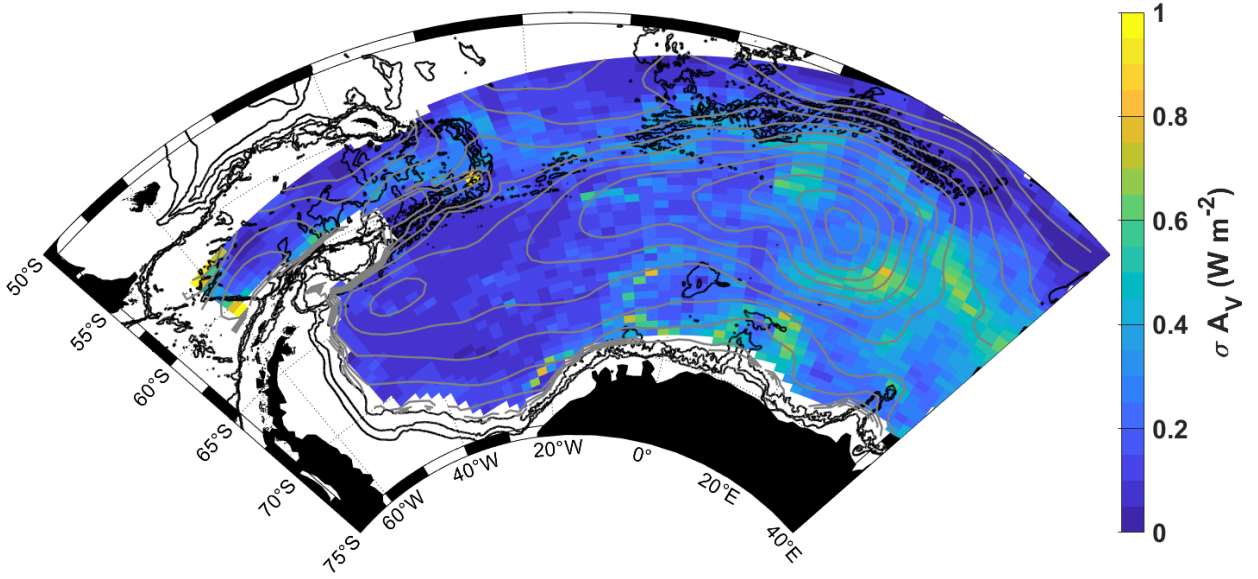
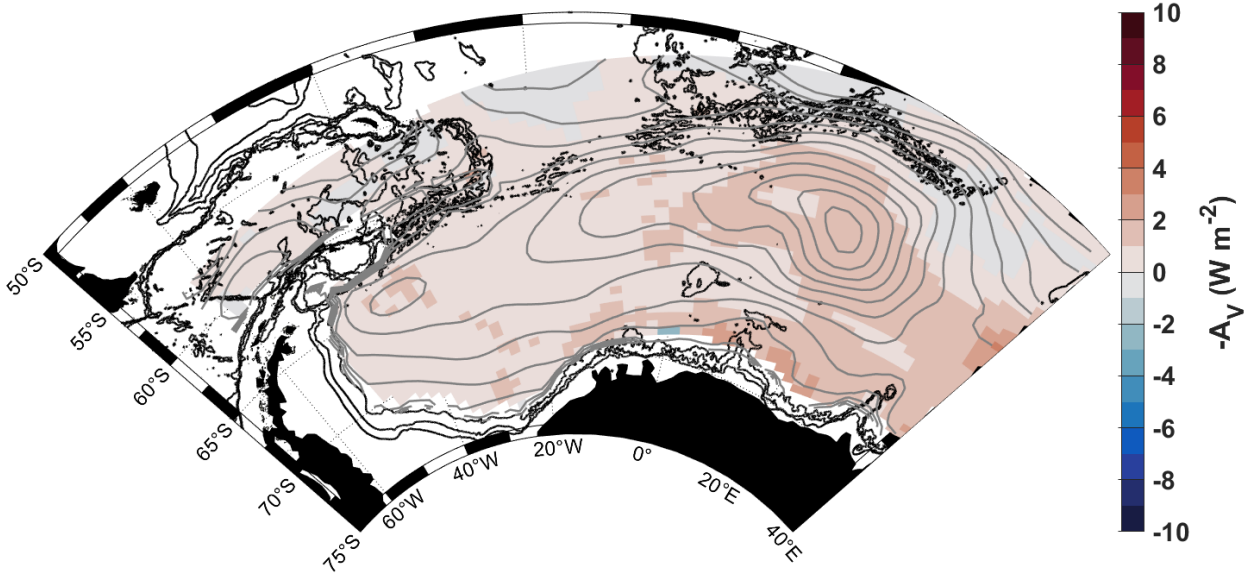


Figure 2: (a) A random sample of vertical profiles of conservative temperature (the position of the profiles are marked by stars in Fig. S1b, the red star marking the position of the example profile in black), where Θ_{\max} is marked by a triangle, the upper boundary (i.e., mid-thermocline) and the lower boundary (mid-thermocline + 1000) are marked by squares, and the upper and lower WDW boundaries (defined by a neutral density range of 28 to 28.27 kg m⁻³) are marked by stars. This is to highlight that our method for the vertical boundary limits allows for the full inclusion of the core of WDW while also excluding Winter Water.

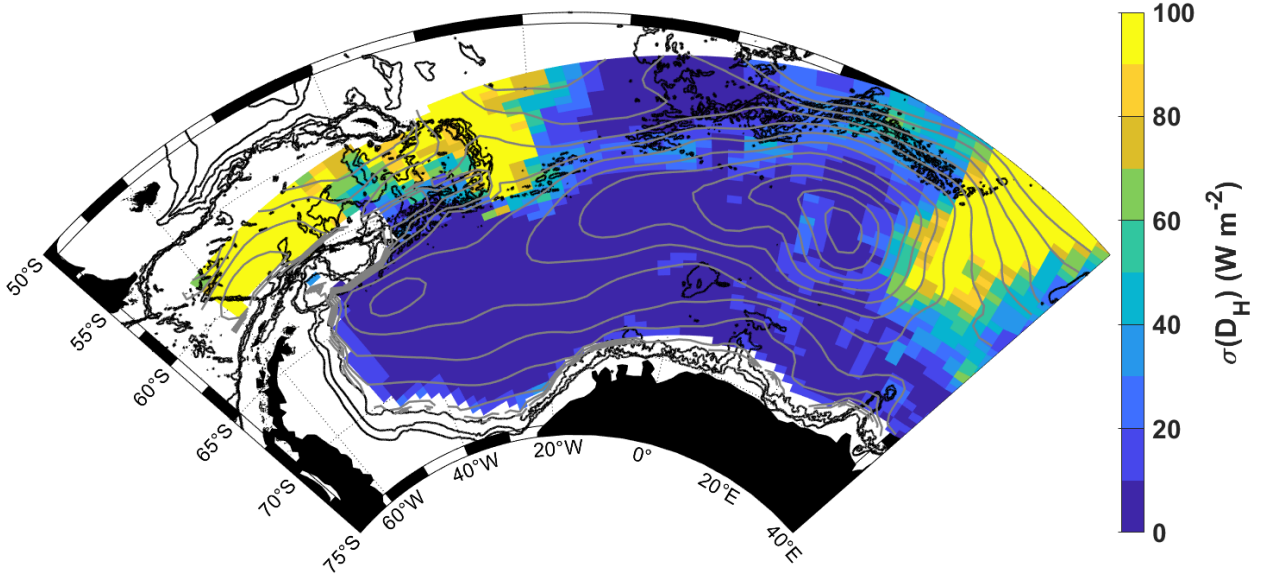
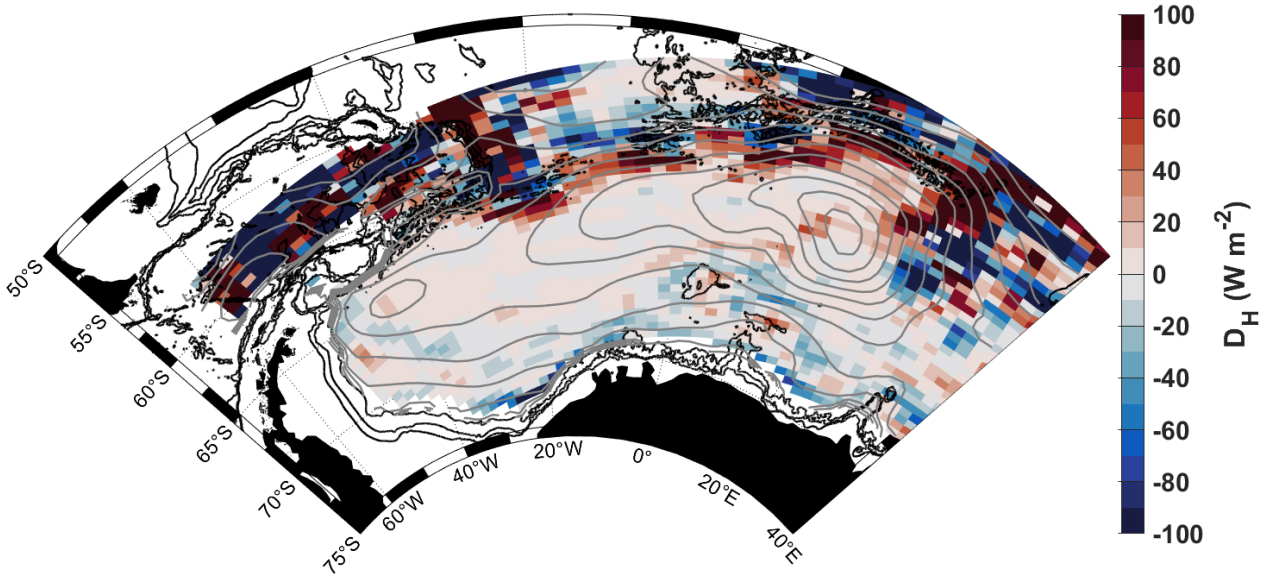
Figure 3: The heat budget terms in W m^{-2} , from Eq. 1.2, for a layer of water 1000 m thick from the depth of the mid-thermocline: (a) mean horizontal geostrophic heat advection, (b) Total propagated error of mean horizontal advection, (c) mean vertical advection, (d) Total propagated error of mean vertical advection, (e) horizontal turbulent diffusion, (f) Total propagated error of horizontal turbulent diffusion, (g) vertical turbulent diffusion, (h) Total propagated error of vertical turbulent diffusion, (i) the sum of the terms in a,c,e,g, and (j) the total propagated error of the sum of the terms. Positive values indicate warming, i.e. heat transport convergence, where more heat is entering the grid cell than is leaving it, whereas negative (blue) values indicate cooling, i.e. heat transport divergence, where more heat is leaving the grid cell than is entering it. Grey and black contours provide the horizontal streamlines and the 1000, 2000 and 3000 m isobaths respectively (as in Fig. 1). Note the different colour scales for the horizontal versus vertical fluxes.



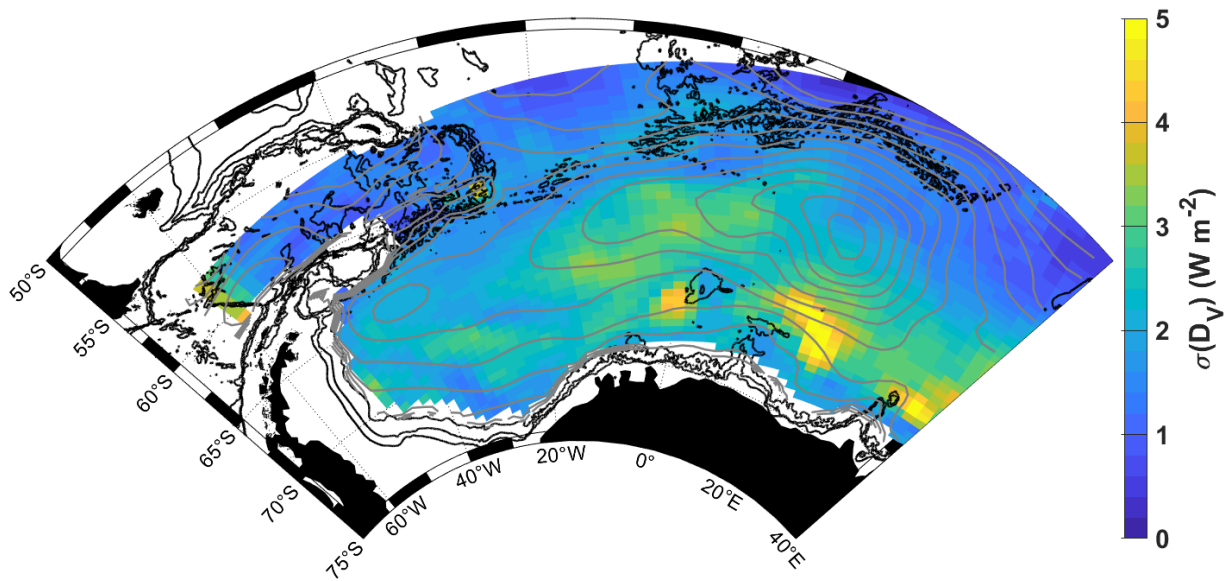
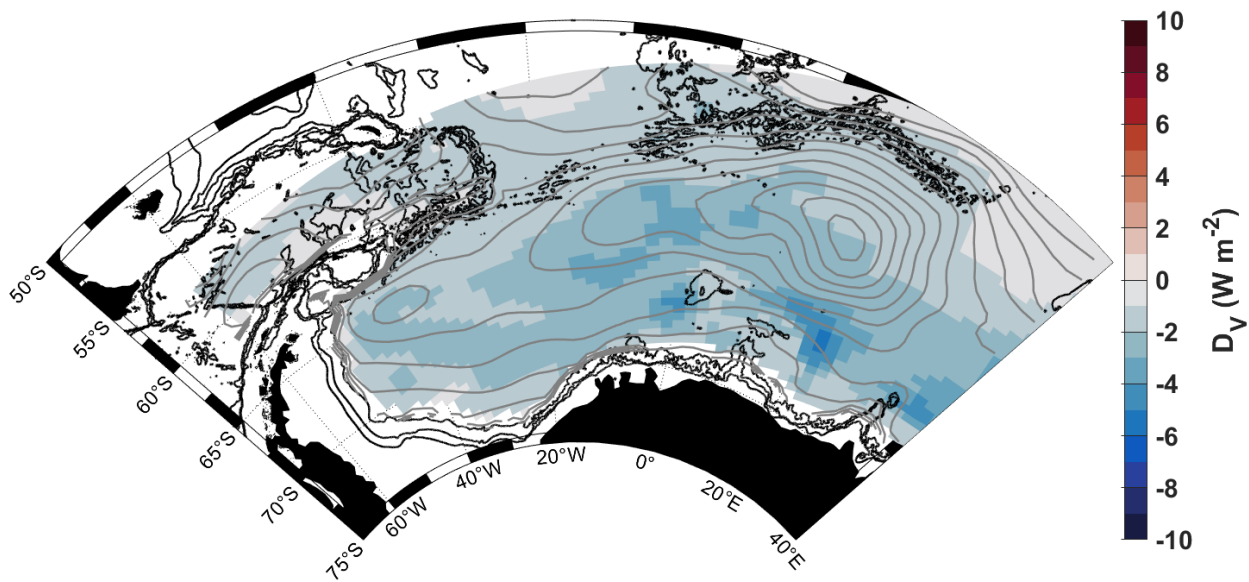
(b)



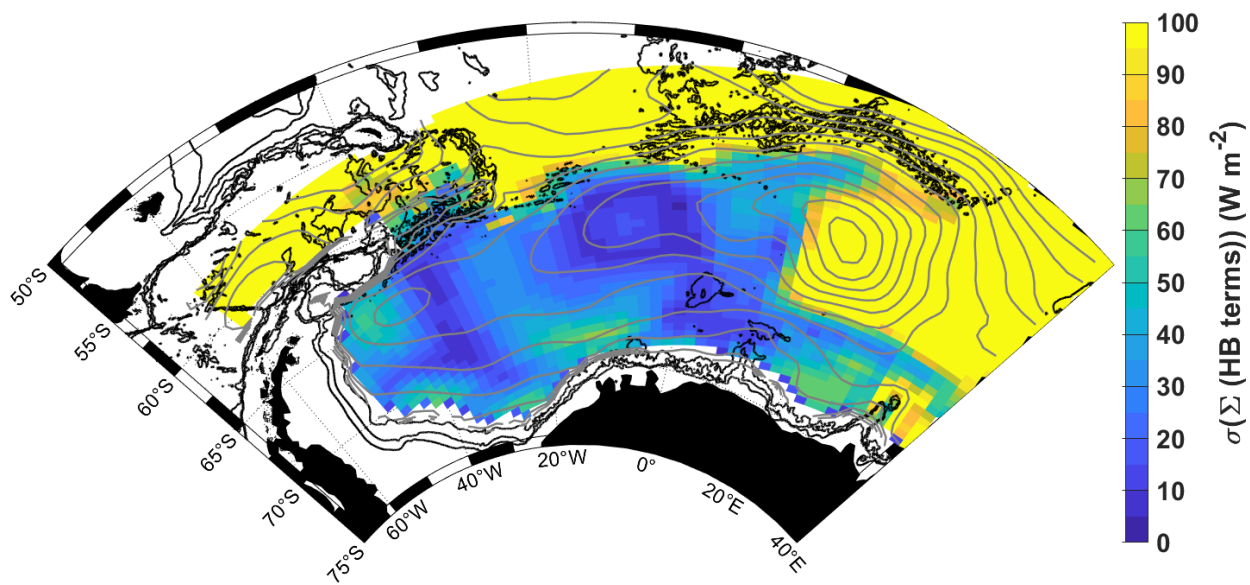
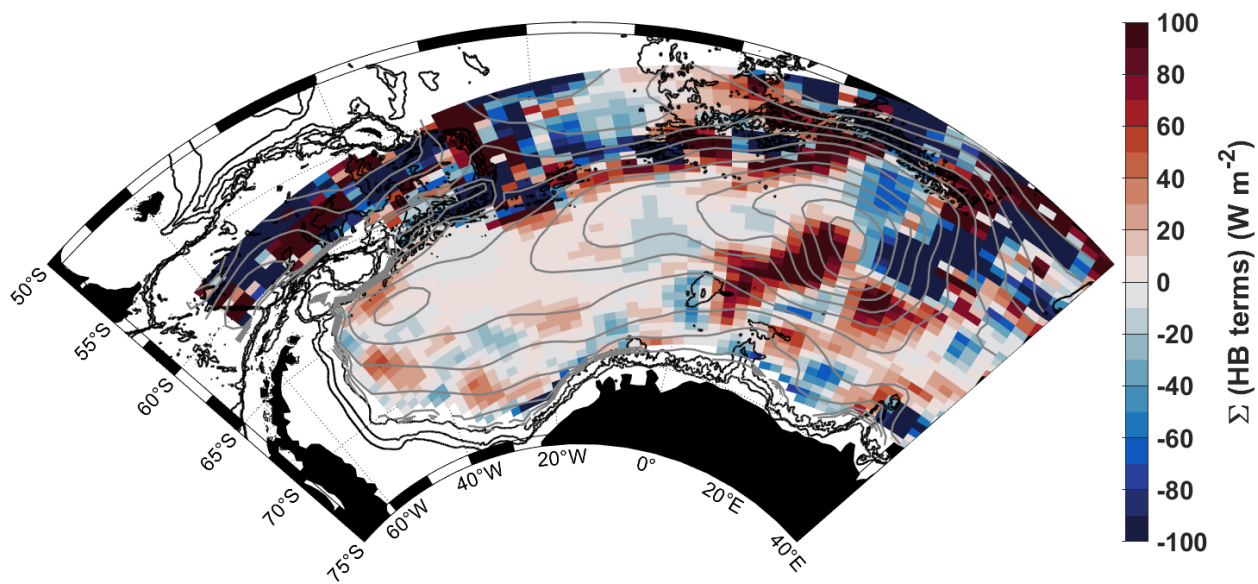
(c)



(d)



(e)



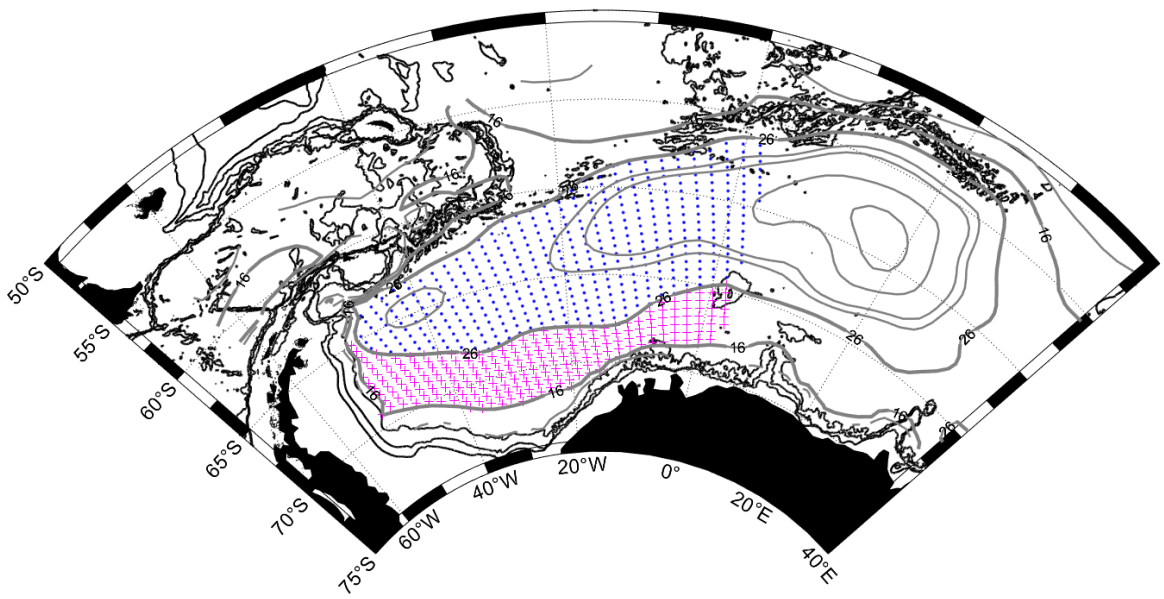


Figure 4: The stippled areas show the regions defined as SL (magenta crosses) and IC (blue dots) respectively, encased in the streamlines used to define the SL and IC regions ($16 < SL < 26$ Sv and $IC > 26$ Sv). These regions are horizontally integrated across in the following Section 4.2. Grey and black contours provide the horizontal streamlines and the 1000, 2000 and 3000 m isobaths respectively (as in Fig. 1).

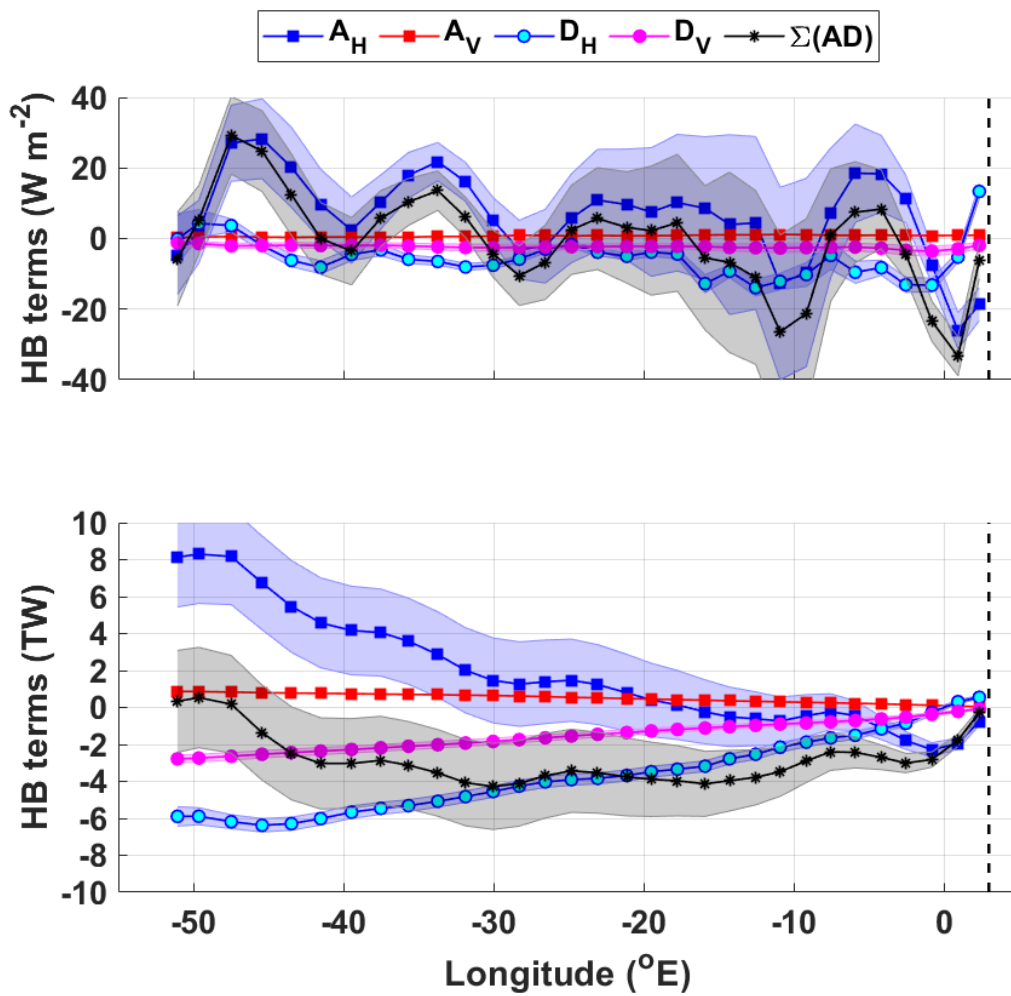


Figure 5: upper panel: the mean heat budget terms for the open southern limb (SL) of the gyre in W m^{-2} ; lower panel: the cumulative heat budget terms in Terawatts (TW). The key for the legend is listed in Table 2. The dashed vertical line marks the approximate longitude of Maud Rise, at 3°E . The shaded errors provide the associated propagated error (detailed in section 3.2 and the supplement). The SL region is marked by magenta stippling in Fig. 4.

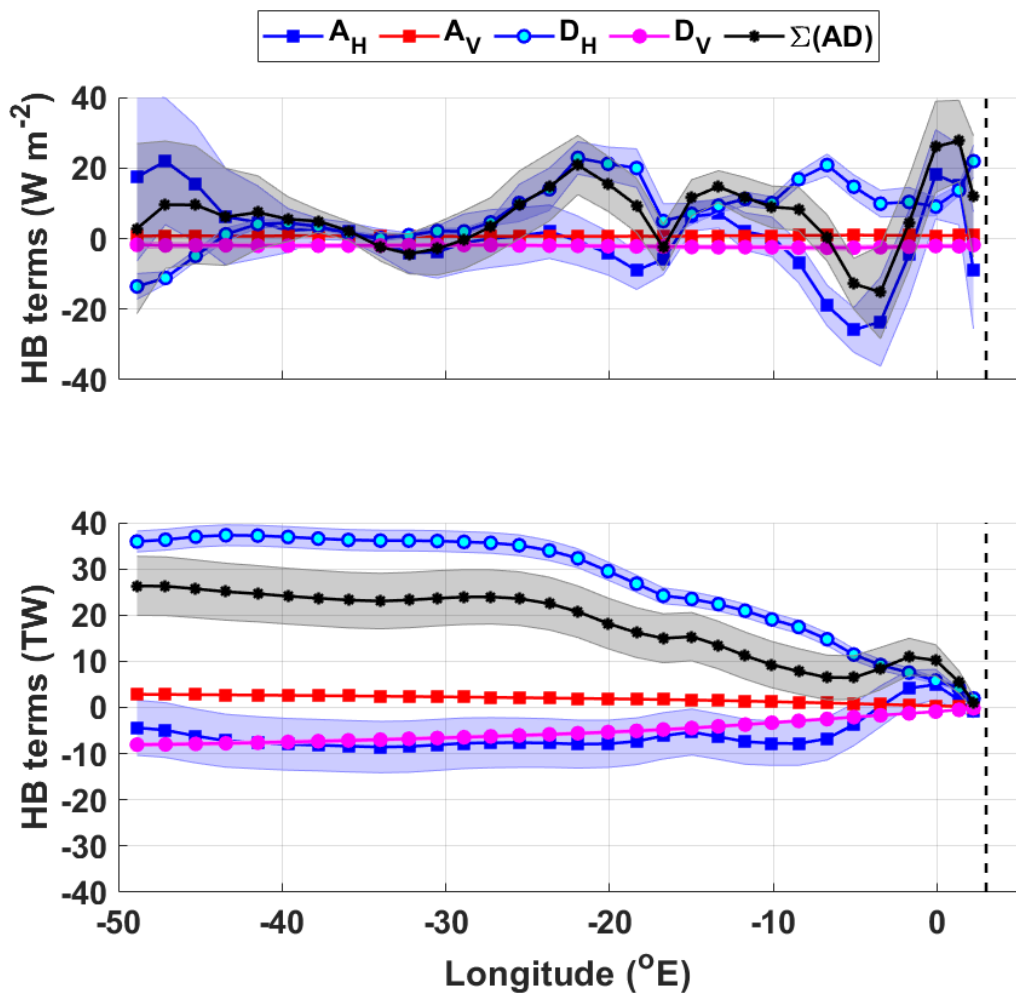


Figure 6: As in Fig. 5, but for the interior circulation cell (IC) of the Weddell Gyre. The IC region is marked by magenta stippling in Fig. 4.

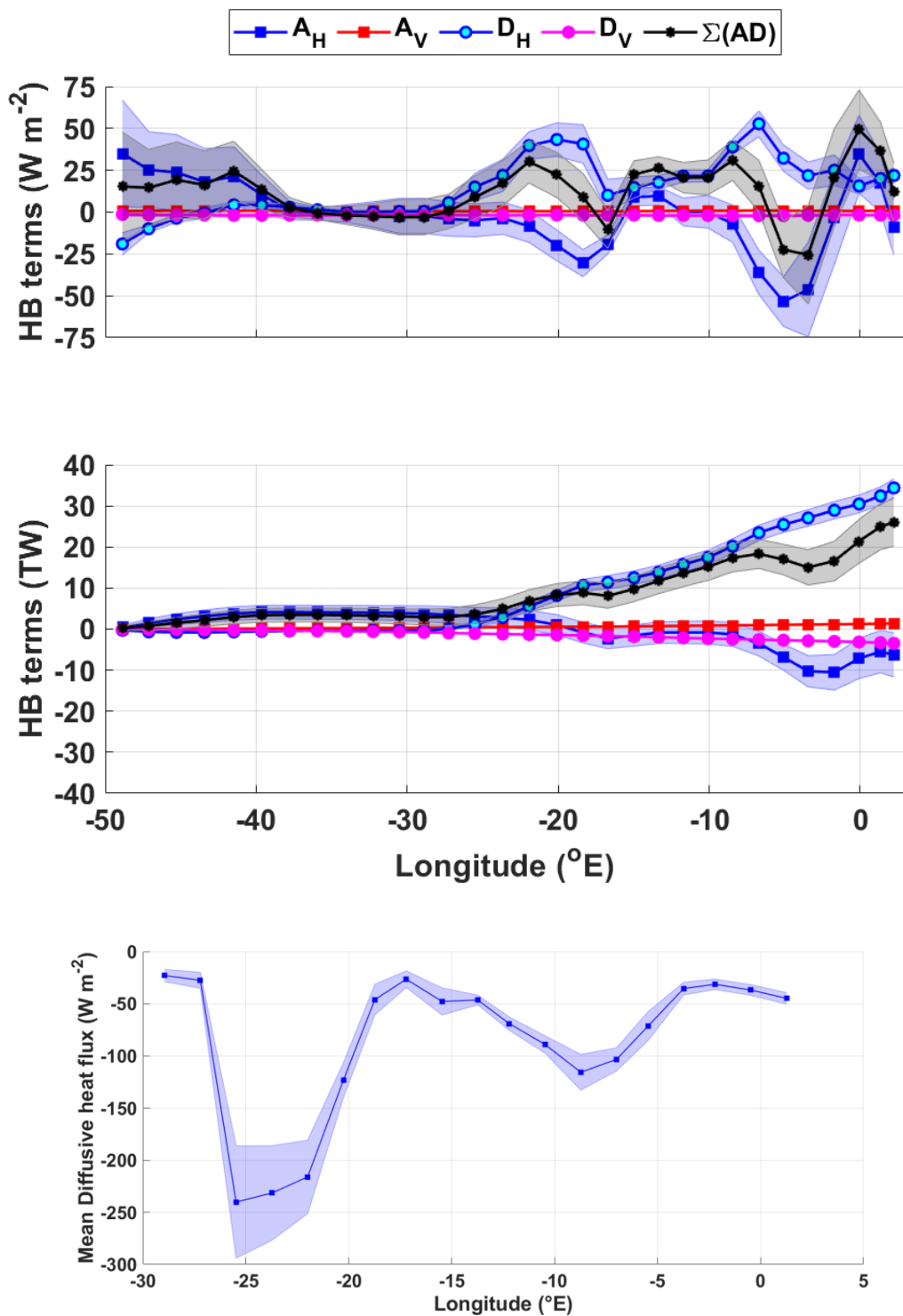


Figure 7: (a) Heat budget terms for the IC-north: upper panel: zonal means in W m^{-2} ; lower panel: the cumulative heat budget terms from west to east in Terawatts (TW). The key for the legend is listed in Table 2. The dashed vertical line marks the approximate longitude of Maud Rise, at 3°E . Panel b shows the zonal variation of the diffusive horizontal heat flux across the northern boundary of the northern limb of the Weddell Gyre, in W m^{-2} , defined by the streamline that equals 26 Sv. Negative values indicate a southward flux of heat into the eastward-flowing northern limb of the Weddell Gyre from north of the northern Weddell Gyre boundary (the subsequent cumulative horizontal diffusive heat flux across the northern boundary is provided in the Supplements in Fig. S6a).

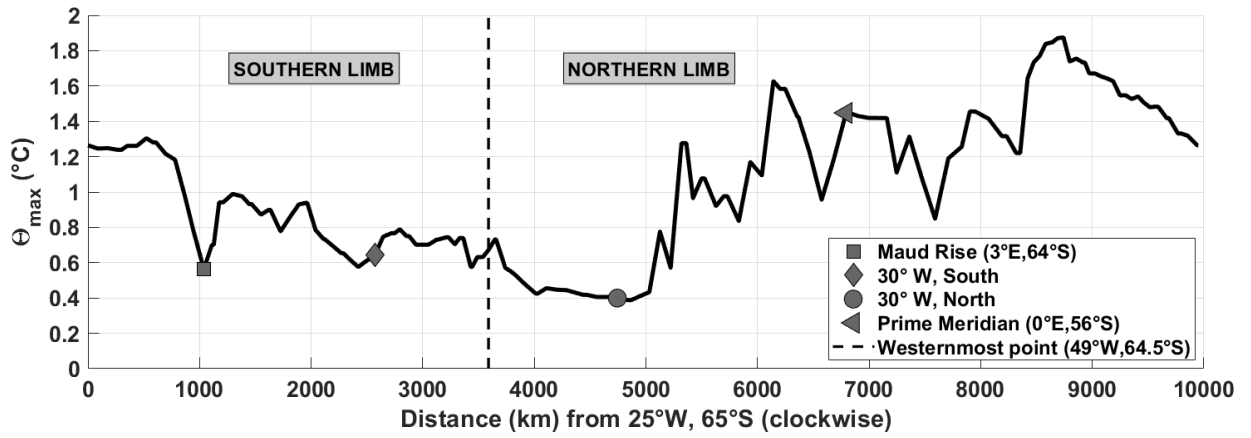
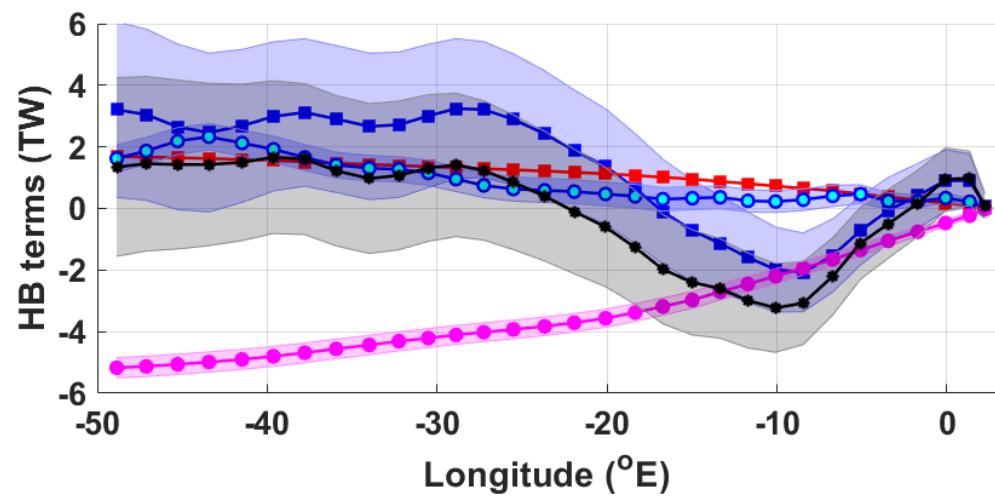
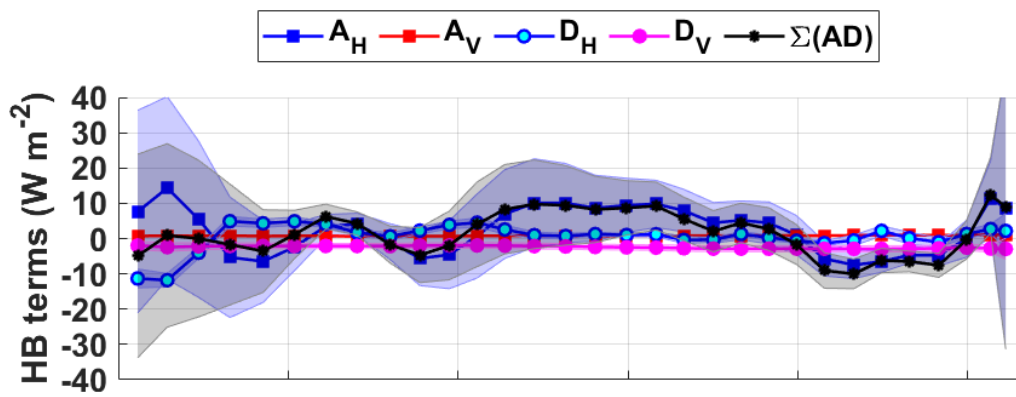


Figure 8: θ_{\max} (°C) along the streamline $\Psi = 26$ Sv (i.e., the IC boundary, labelled in Fig. 4). The distance in km is along the streamline in a clockwise direction from 25°W, 65°S, with key locations marked using the legend.



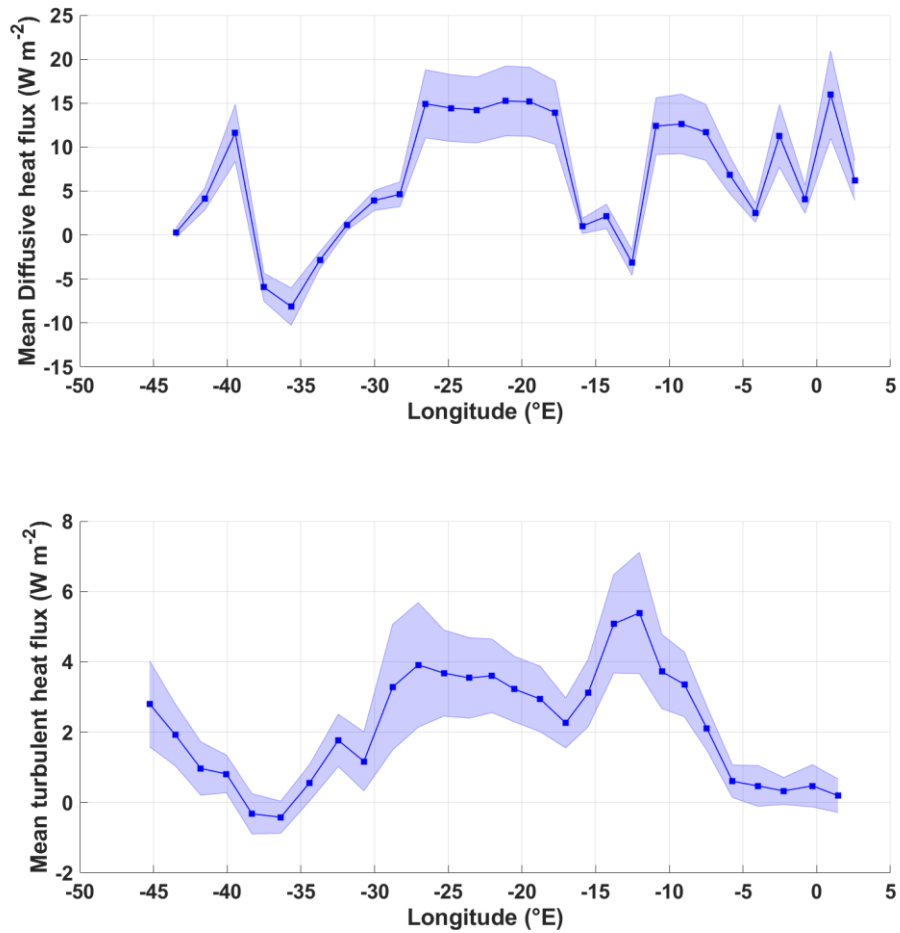


Figure 9: (a) Heat budget terms for the IC-south, west from $\sim 3^{\circ}\text{E}$ (Maud Rise): upper panel: the heat budget terms in W m^{-2} ; lower panel: the cumulative heat budget terms in Terawatts (TW). The key for the legend is listed in Table 2. Panels b and c show the zonal variation of the diffusive horizontal heat flux in W m^{-2} for (b) across the boundary between the SL and the IC, where the streamline is 26 Sv, and (c) across the central gyre axis from the IC-south to the IC-north. Positive values indicate a northward flux of heat from the SL into the IC, and from the IC-south northwards into the IC-north, respectively (the subsequent cumulative horizontal diffusive heat flux across the northern boundary is provided in the Supplements in Fig. S6b-c).

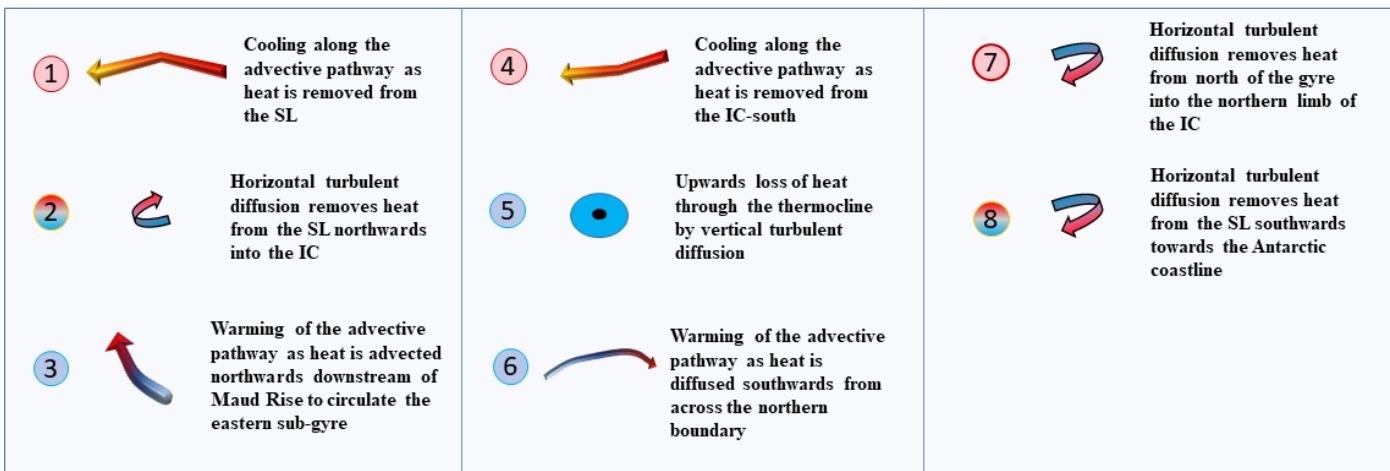
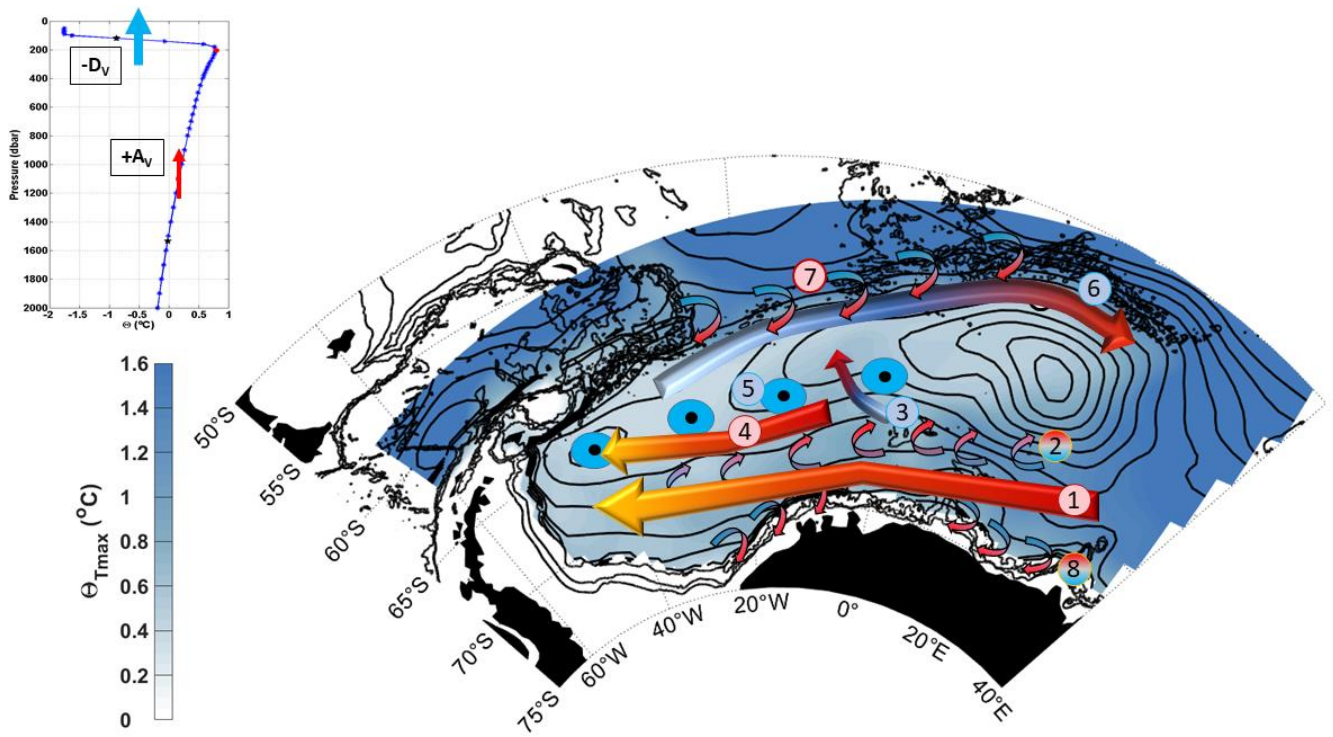


Figure 10: Schematic of proposed mechanisms by which heat is transported throughout the Weddell Gyre, based on interpretation of results in Sections 4 & 5.2. The blue-scale colour shading shows Θ_{\max} and the black contours show the stream function with 5 Sv spacing, as in Fig. 1. The numbered keys assigned to each feature (arrows and circles) are described in panel b and Table 4. Where the colour of the number and feature are red, heat flux convergence (heat source) is indicated, and where they are blue indicates heat flux divergence (heat sink). The horizontal turbulent diffusive fluxes, indicated by small curved arrows (2,7,8), change from blue to red to indicate a direction of heat flux. The upper left inset shows an example of the vertical temperature profile, with $-D_V$ indicating a vertical diffusion of heat upwards out of the layer through the thermocline, and $+A_V$ indicating a vertical advection of heat upwards into the layer from below.

Table 1. A summary of the associated data source, method and citation for each variable required in the heat budget (Eq. 1.2 in Section 3, and column 2 below).

Section for details	Variable	Data source	Methodology	Citation
2.2	Gridded Temperature (θ)	Argo floats (2002-2016)	Objective mapping	Reeve et al., 2016
2.2	Gridded horizontal velocity (U)	Argo floats (2002-2016)	Objective mapping, cost function	Reeve et al., 2019
2.2	Long-term mean velocity at the shelf edge (U)	Moorings (1989-2016)		Le Piah et al., 2020
2.2	Bathymetry	GEBCO		IOC et al., 2003
S3	Vertical (Ekman) velocity (w_E)	ERA5-interim reanalysis and Polar Pathfinder (listed below)	Regridded using a distance-weighted mean	Hersbach et al., (2020) & Tschudi et al., (2019)
S3	Wind stress ($\tau_{\text{air-ocean}}$) derived from wind field at 10 m above sea surface (U_{10})	ERA5-interim reanalysis	Used to compute w_E	Hersbach et al., (2020)
S3	Sea-ice concentration (α)	ERA5-interim reanalysis	Used to compute w_E	Hersbach et al., (2020)
S3	Sea-ice velocity (U_{ice})	Polar Pathfinder Daily 25 km EASE-Grid Sea Ice Motion Vectors	Used to compute w_E	Tschudi et al., (2019)
3 & S4	Horizontal diffusivity (κ_H)	Sevellec et al., (2022), and estimates in the literature (see citation)	Where available (i.e., outskirts of gyre) the Sevellec dataset. Infilled within gyre with a constant value based on the literature	Sevellec et al., 2022; Donnelly et al. (2017); Zika et al. (2009) & Cole et al., (2015)
3	Vertical diffusivity (κ_V)	Based on estimates in the literature (see citation)		Donnelly et al. (2017), Zika et al. (2009) & Cole et al., (2015)
S2	Air-sea heat fluxes	ERA-interim reanalysis		Jones et al., 2016

Table 2: Explanations of the abbreviations used in Figs. 3-8.

Term	Description
A_H	Mean horizontal geostrophic heat advection
A_V	Mean vertical heat advection
D_H	Horizontal turbulent diffusion
D_V	Vertical turbulent diffusion
$\sum AD$	The sum of the heat budget terms in Eq. 1, listed above, where A stands for the horizontal and vertical advection terms and D stands for the horizontal and vertical diffusion terms.

Table 3: Zonal mean ($W m^{-2}$) and net (TW) heat budget contribution of the different terms in Eq. 1.2 for the SL and IC zones of the Weddell Gyre (Fig. 3 and 4 respectively), and an estimate of temperature change (dT/dt), using a time period of 14 years. The uncertainty provided for the net heat budget terms (in TW) are the sum in quadrature of the propagated errors. For the mean heat budget terms (in $W m^{-2}$), the provided uncertainty is the standard deviation of the zonal mean heat budget term, and the mean error (in $W m^{-2}$) is the mean of the propagated error and the standard deviation of the mean propagated error. See Section 5.2 for further information.

Heat Budget Term	SL			IC		
	Mean ($W m^{-2}$)	Mean Error ($W m^{-2}$)	Net (TW)	Mean ($W m^{-2}$)	Mean Error ($W m^{-2}$)	Net (TW)
Mean Air-Sea flux	-2.5		-3	+8		+27
Mean horizontal advection	+6 ± 13	13 ± 7	+8 ± 3	+0.2 ± 11	9 ± 5	-4 ± 6
Mean vertical advection	+0.7 ± 0.3	0.1 ± 0.04	+0.9 ± 0.02	+0.8 ± 0.1	0.04 ± 0.01	+2.8 ± 0.03
Horizontal turbulent diffusion	-5.5 ± 5.7	2 ± 1	-6 ± 0.5	+7.8 ± 9	3 ± 2	+36 ± 2
Vertical turbulent diffusion	-2.3 ± 0.5	1 ± 0.2	-2.8 ± 0.2	-2.1 ± 0.3	0.6 ± 0.1	-8 ± 0.4
Heat tendency (i.e., sum of the heat budget terms)	-0.9 ± 14	13 ± 7	+0.3 ± 3	+6.7 ± 10	9 ± 5	+26 ± 6
Temperature tendency over 14 years ($^{\circ}C$)			+ 0.03 ± 0.2 $^{\circ}C$ or +0.002 ± 0.02 $^{\circ}C/yr$			+ 0.8 ± 0.2 $^{\circ}C$ or 0.06 ± 0.01 $^{\circ}C/yr$

Table 4: Summary of the key heat budget terms that are shown in the schematic in Fig. 8. The numbers correspond to the number key in Fig. 8, and the associated features in the schematic. Abbreviations used for the heat budget terms are defined in Table 2.

Key	Process	Net heat budget contribution (TW)
1	A_H into SL	$+8 \pm 3$ TW
2	D_H out of SL (into IC-south)	-6 ± 0.5 TW (into IC-south: $\sim 1.1 \pm 0.1$ TW)
3	A_H out of IC-south (West of MR and East of 10°W ; i.e., circulating eastern sub-gyre)	-2 ± 1.4 TW
4	A_H into IC-south (downstream of MR)	5 ± 3 TW
5	D_V out of IC-south	-5 ± 0.3 TW
6	A_H out of IC-north	-6 ± 5 TW
7	D_H into IC-north from ACC	34 ± 2 TW (direct flux across northern boundary is $\sim 17 \pm 1$ TW, suggesting half exits the eastern end of the IC-north layer)

Figures for Supplements

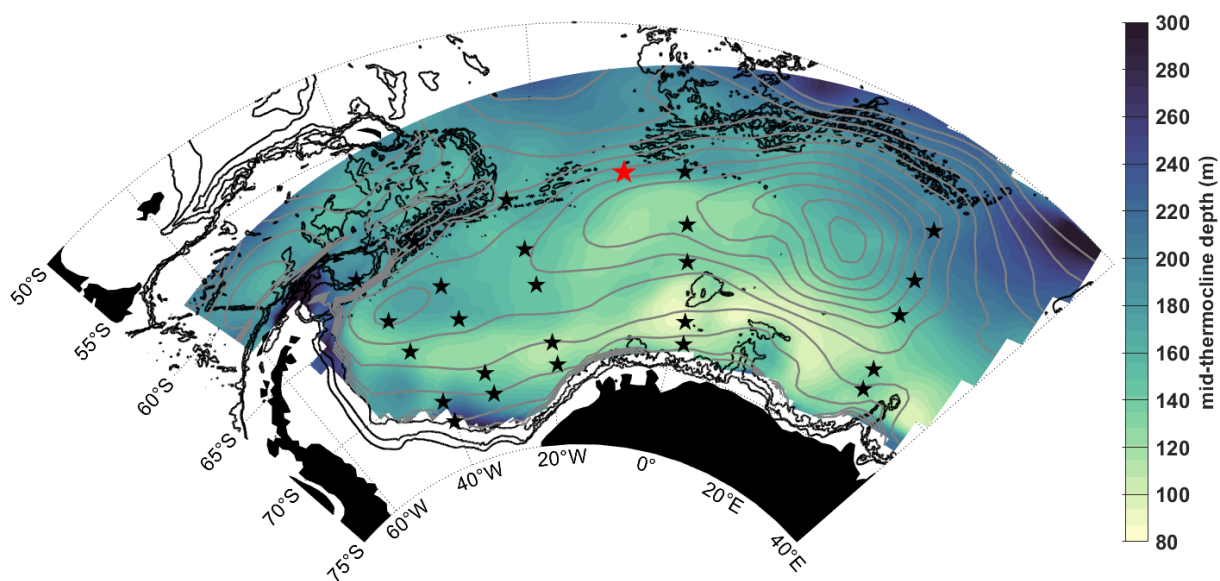


Figure S1: Upper boundary depth (m), defined as the mid-thermocline, with stars marking the positions of profiles plotted in Fig. 2, and streamlines (grey contours) of the vertically integrated stream function for 50-2000 dbar with a spacing of 5 Sv, derived from in-situ observations from Argo floats (Reeve et al., 2019, 2016), as in Fig. 1. The black contours show the 1000, 2000 and 3000 m isobaths, from the general bathymetric chart of the oceans (GEBCO, IOC et al., 2003).

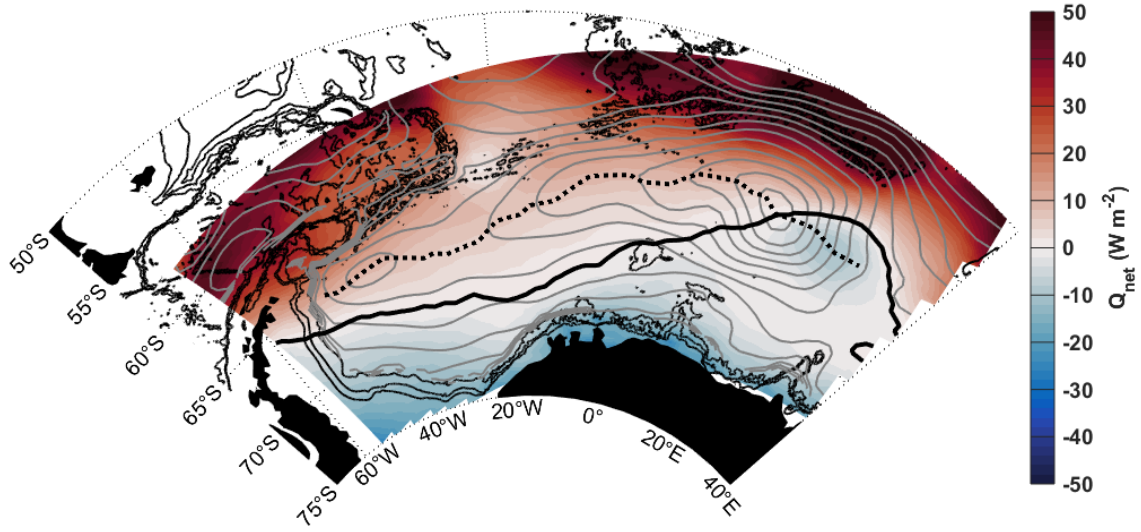


Figure S2: Net air-sea heat flux (i.e. the sum of long/short-wave radiation, latent and sensible heat fluxes, in W m^{-2}): long-term mean from 2002 to 2016, from ERA-interim reanalysis data. Positive values indicate heat flux into the ocean. The thick black line indicates the zero-contour line for Q_{net} . The central gyre axis is indicated by the dashed black line, defined as the meridional maximum stream function value. South of the dashed line the flow of the water column is westward and flow north of the dashed line is eastward. Streamlines (grey contours) show the vertically integrated stream function for 50-2000 dbar with a spacing of 5 Sv, derived from in-situ observations from Argo floats (Reeve et al., 2019, 2016), as in Fig. 1. The black contours show the 1000, 2000 and 3000 m isobaths, from the general bathymetric chart of the oceans (GEBCO, IOC et al., 2003).

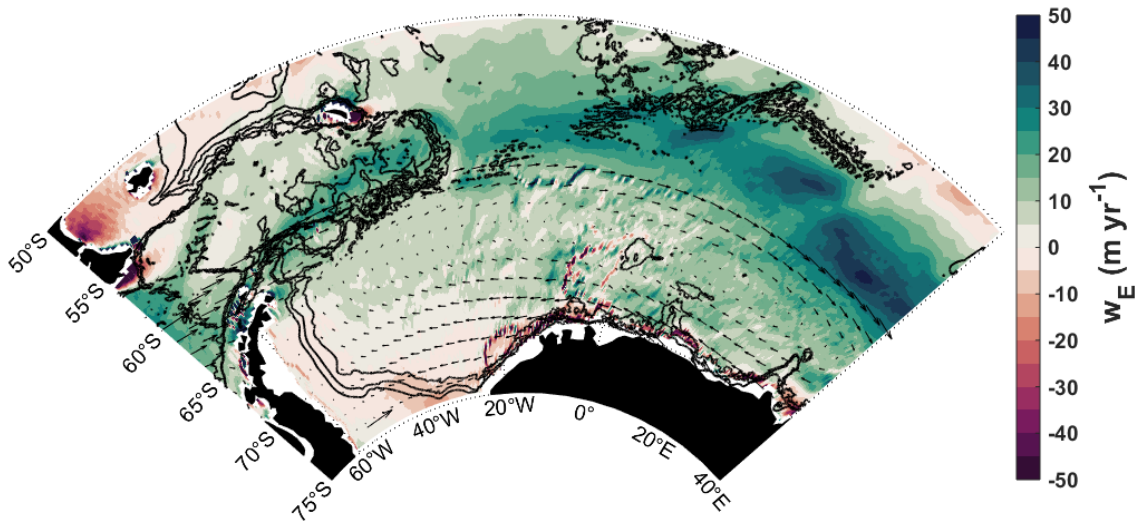
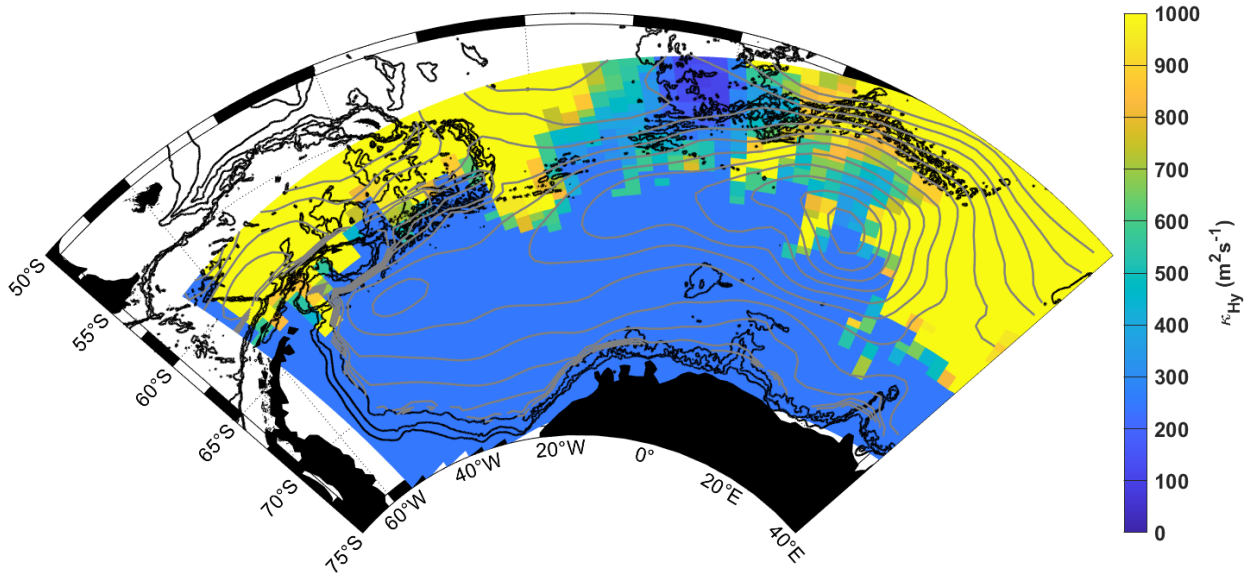
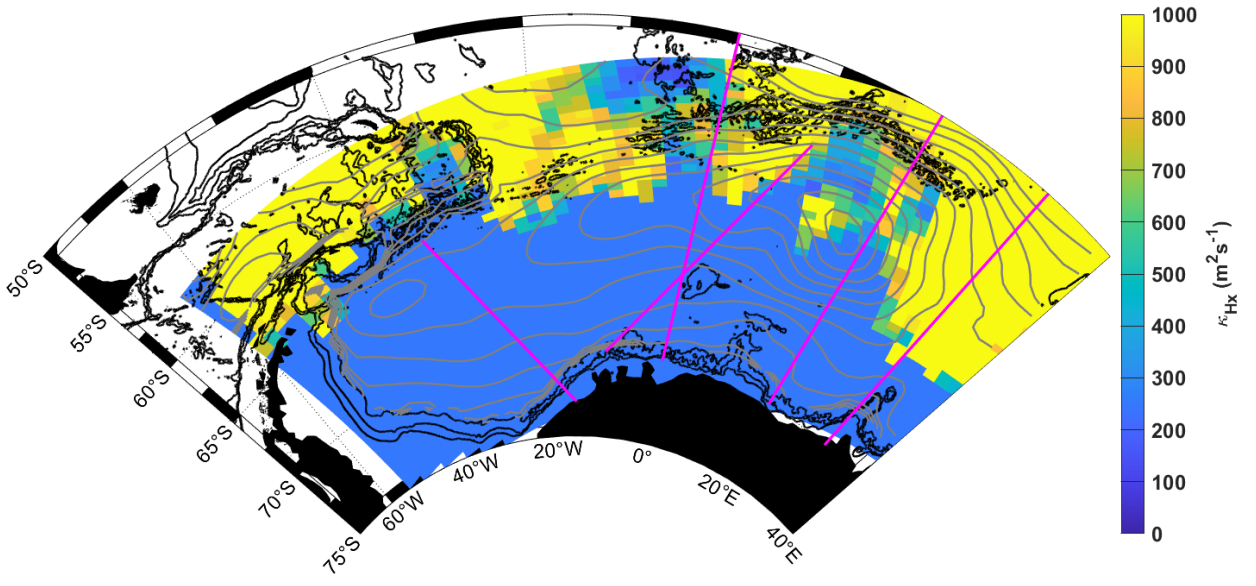


Figure S3: Mean 2002-2016 vertical Ekman pumping velocity (w_E : m/year), from Era-interim ECMWF reanalysis (ERA5 monthly mean output; Hersbach et al., 2020) and sea-ice velocity from Polar Pathfinder Daily 25 km EASE-Grid Sea Ice Motion Vectors (Tschudi et al., 2019), where positive values indicate upwelling. Black arrows show surface wind stress (N m^{-2}), south of 60°S (in order to emphasise the weaker surface wind stress within the Weddell Gyre region, which would disappear if we were to include the much stronger wind stress over the ACC); the arrow at 50°W , 74°S is 0.05 N m^{-2} . The black contours show the 1000, 2000 and 3000 m isobaths, from the general bathymetric chart of the oceans (GEBCO, IOC et al., 2003).



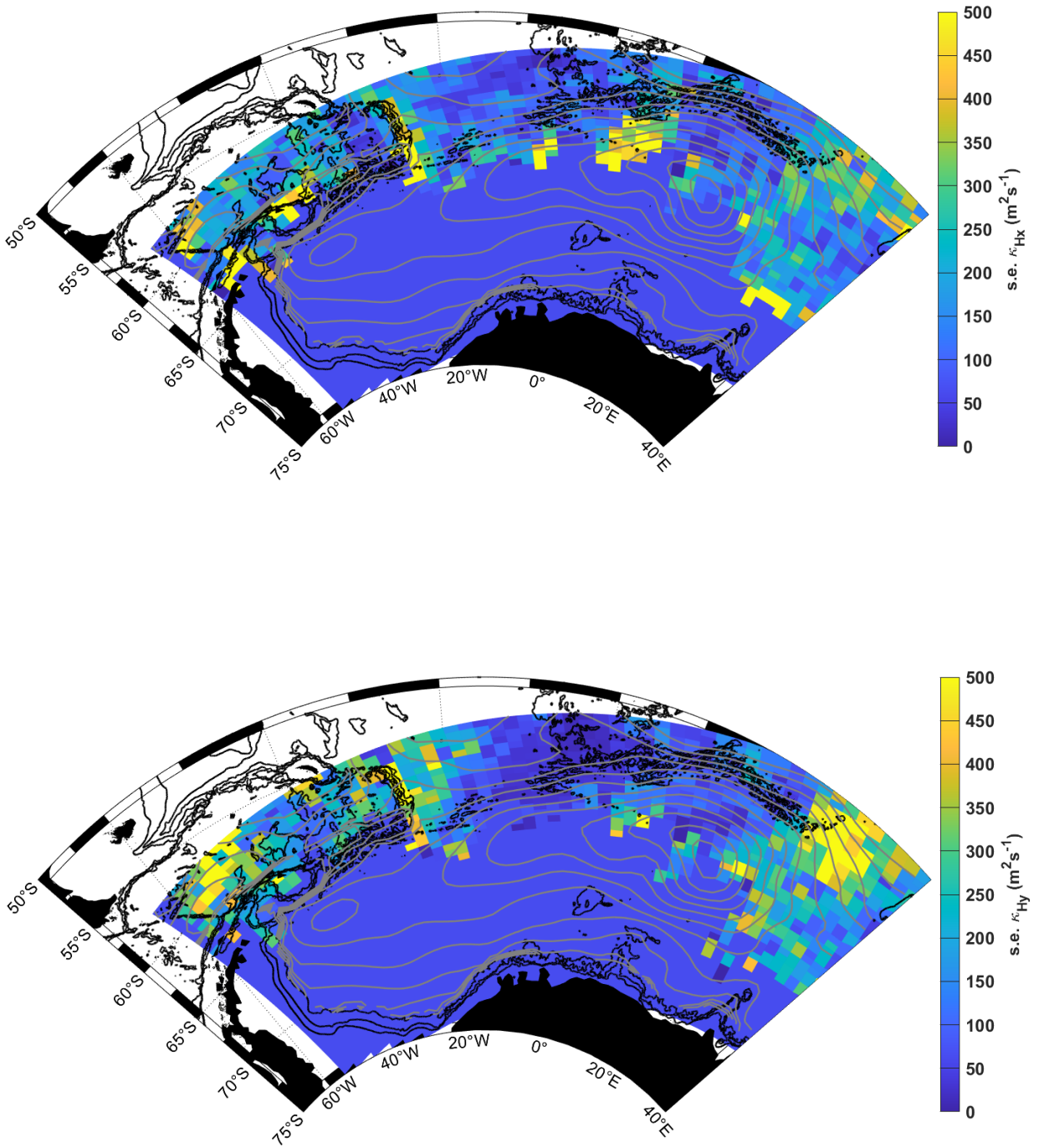


Figure S4: Horizontal diffusivity as a combination of the Sevellec et al. (2022) dataset and infilling with a background value of $247 \pm 63 \text{ m}^2 \text{ s}^{-1}$, from Donnelly et al. (2017). The upper panels show the zonal and meridional components from left to right, whereas the lower panels show their corresponding standard errors respectively. In the upper left panel, magenta lines mark the approximate positions of the ship-based data used in Donnelly et al., (2017).

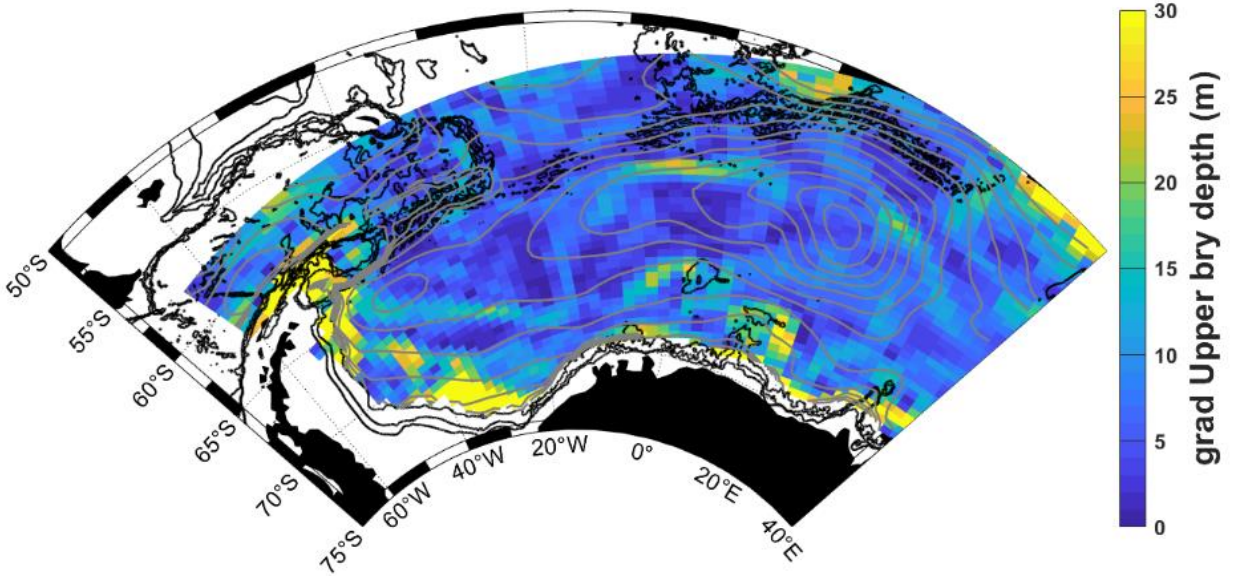
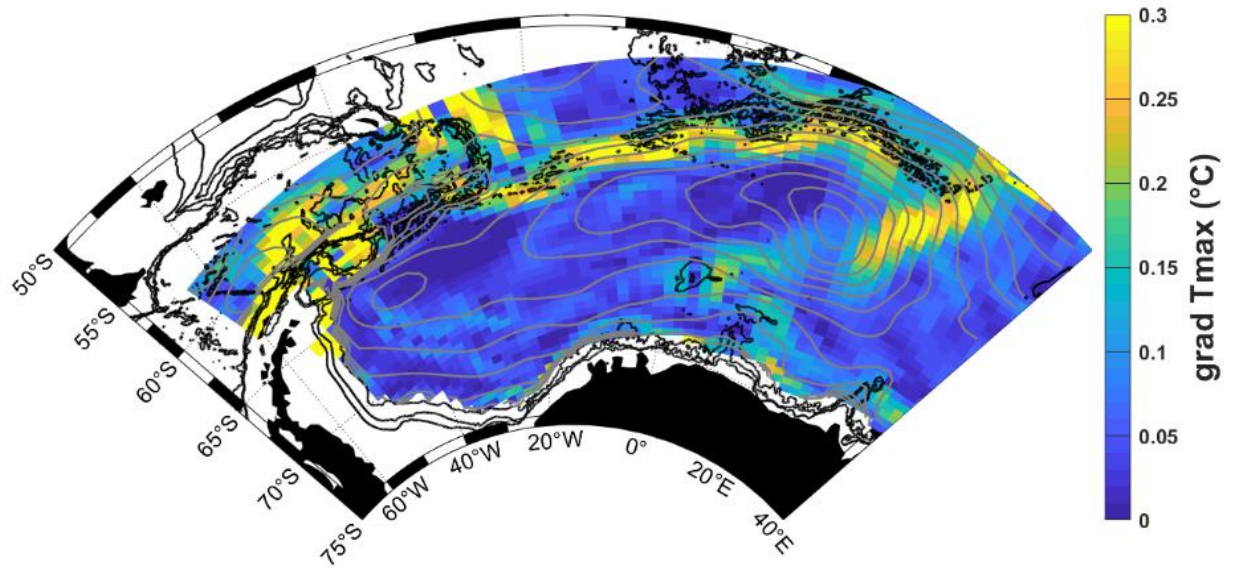


Figure S5: (a) Horizontal gradient in the upper boundary depth (i.e. mid-thermocline depth; m), and (b) horizontal gradient in the sub-surface temperature maximum ($^{\circ}\text{C}$).

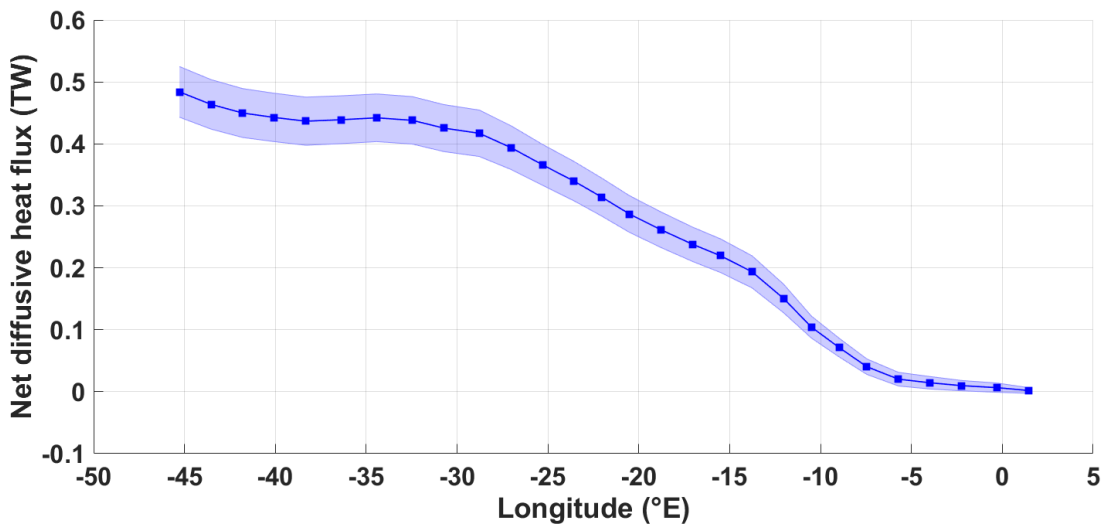
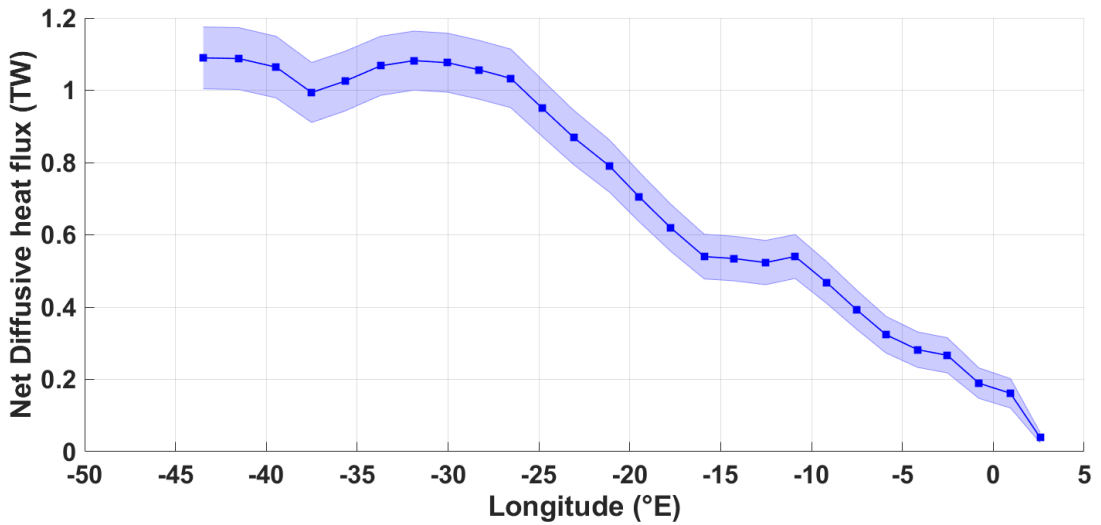
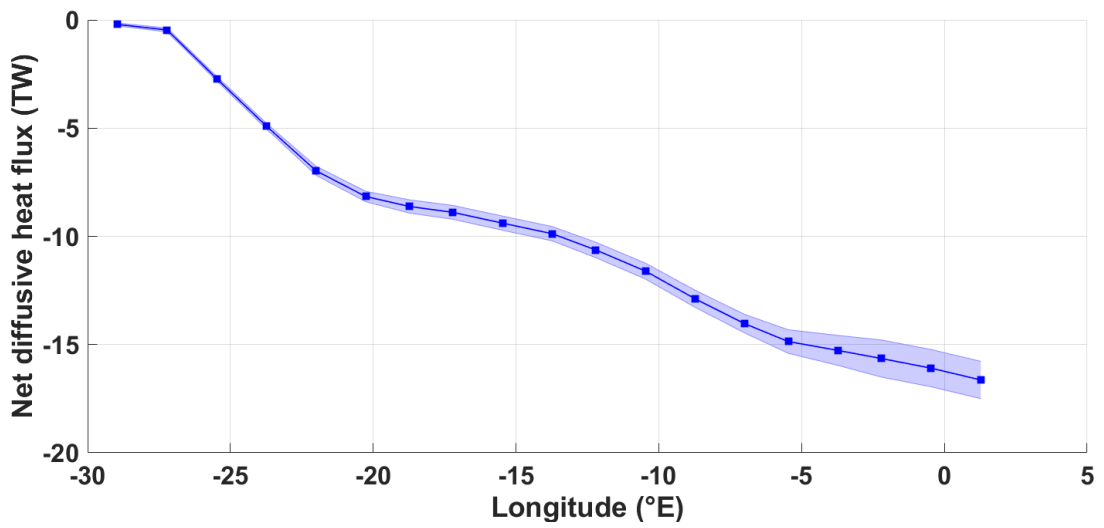


Figure S6: the cumulative sum of the diffusive heat flux in TW. (a) across the northern gyre boundary from west to east, where negative values indicate a southward flux of heat into the eastward-flowing northern limb of the Weddell Gyre from north of the northern Weddell Gyre boundary; (b) along the boundary between the southern inflow limb and IC-south, from east to west, where positive values indicate a removal of heat from the open southern limb of the gyre into the interior; in other words, a northward flux of heat from the southern limb into the interior circulation cell; (c) across the central gyre axis from IC-south to IC-north, where positive values indicate a diffusive heat flux northwards across the gyre axis. Errors are computed following the same method outlined in Section 3.2 and S7, with the cumulative net sum error summed in quadrature (i.e., the square root of the cumulative sum of the squared error).

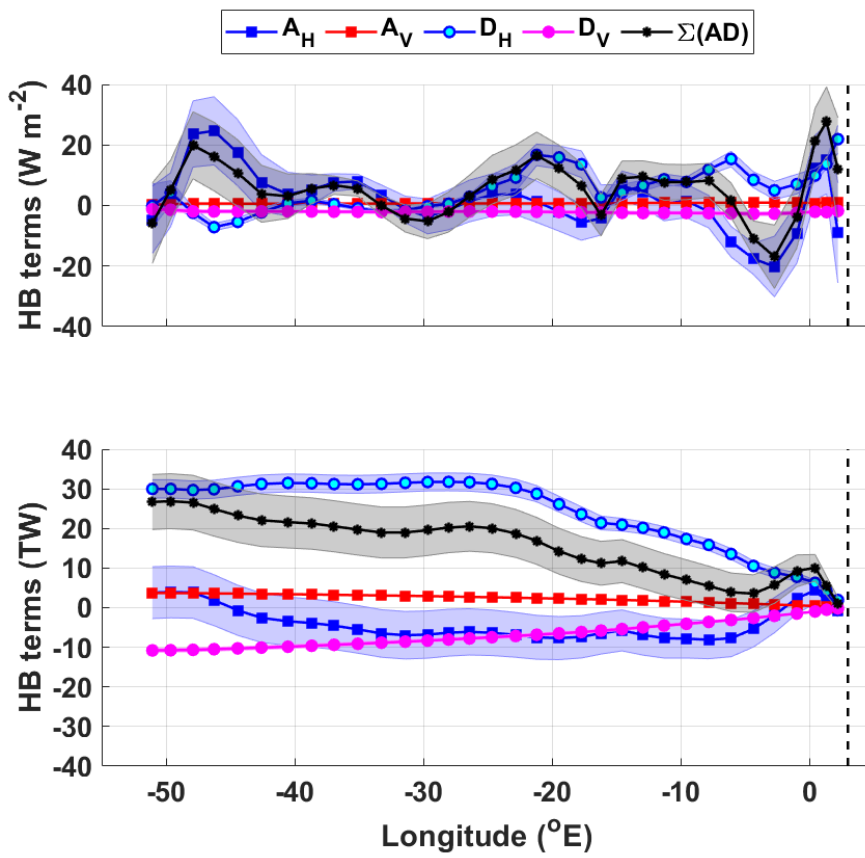


Figure S7: upper panel: the zonal mean heat budget terms, in Wm^{-2} , for the whole Weddell Gyre west of 3°E ; lower panel: the corresponding cumulative heat budget terms in Terawatts (TW). The key for the legend is listed in Table 2. The dashed vertical line marks the approximate longitude of Maud Rise, at 3°E . The shaded errors provide the associated propagated error (detailed in section 3.2 and the supplement). The total region is marked by both blue and magenta stippling in Fig. 4.

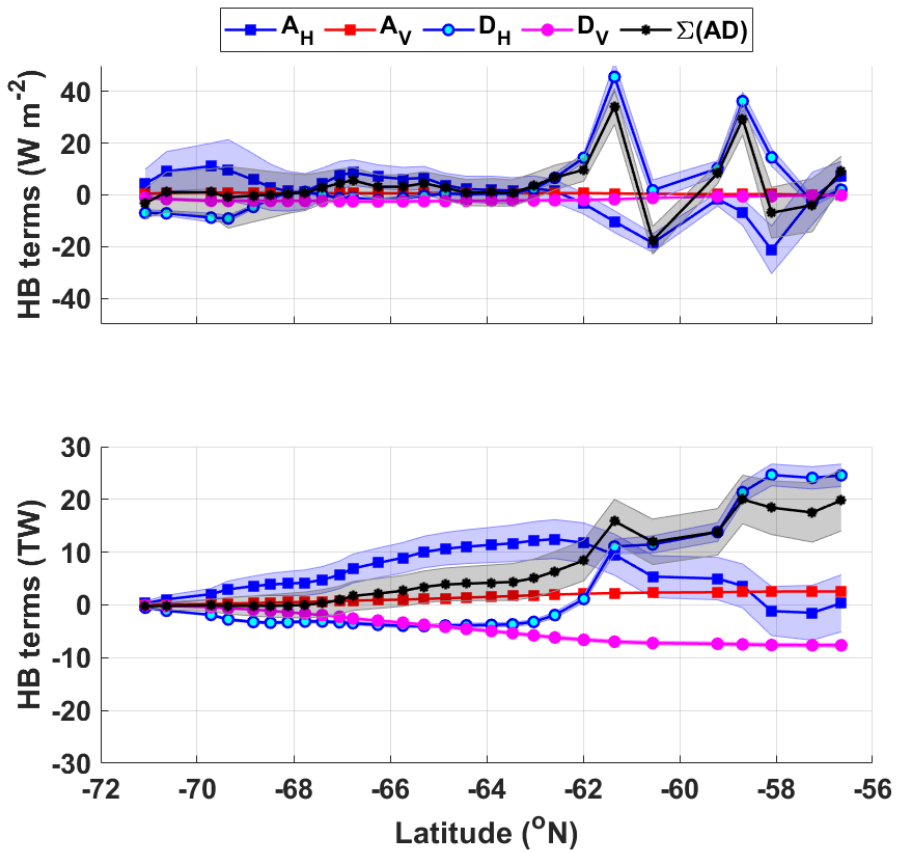


Figure S8: upper panel: the meridional mean heat budget terms, in Wm^{-2} , for the whole Weddell Gyre west of 3°E ; lower panel: the corresponding cumulative heat budget terms in Terawatts (TW). The key for the legend is listed in Table 2. The dashed vertical line marks the approximate longitude of Maud Rise, at 3°E . The shaded errors provide the associated propagated error (detailed in section 3.2 and the supplement). The total region is marked by both blue and magenta stippling in Fig. 4.